THE INFLUENCE OF FRAGMENTATION MODELS ON THE DETERMINATION OF THE STRONG COUPLING CONSTANT α_s IN e^+e^- ANNIHILATION INTO HADRONS

W.de Boer
Max Planck Institut für Physik und Astrophysik
Föhringer Ring 6, D-8000 Munich 40

Abstract:
Hadronic events obtained with the CELLO detector at PETRA were compared with first order QCD predictions using two different models for the fragmentation of quarks and gluons, namely the Hoyer model and the Lund model. In the Lund model the hadrons are formed along strings between quarks and gluons, in the Hoyer model each parton fragments independently according to the Field-Feynman prescription. Several methods have been used to determine the strong coupling constant α_s. With the Hoyer model we find α_s values between 0.15 and 0.20, depending on the method used. With the Lund model we find α_s between 0.24 and 0.28. The difference in α_s with the two models is for a large part due to the different fragmentation schemes and the different treatment of the gluons. A gluon spin test has been performed with both models by comparing first order QCD predictions for the parton thrust with the data.

1. Introduction

The observation of planar 3 jet events in e^+e^- annihilation[1] into hadrons are attributed to the QCD process:

$$e^+e^- \to q\bar{q}g \tag{1}$$

The cross section for this process is determined by the strong coupling constant α_s, which is the only free parameter in QCD. However, QCD deals with quarks and gluons and experiments only observe final state hadrons. Therefore, to determine α_s, one needs models, which relate the $q\bar{q}g$ cross-section to the observed final hadrons.

The CELLO collaboration has studied[2] the influence of the fragmentation models on the determination of α_s by using two rather different models, namely the string fragmentation model of the LUND group[3] (LM) and the Monte Carlo by Hoyer et al.[4] (HM). In the latter model the partons do not fragment along strings, but each parton fragments independently according to the Field-Feynman[5] (FF) prescription. Both generators correspond to first order QCD.

We have used several methods to determine α_s and found that even observables advertised to be "fragmentation independent" give significantly different values of α_s for the two different fragmentation models.

The paper is organized as follows: we first describe the methods to determine α_s (section 2); then follows a description of the fragmentation models (section 3). Sections 4 - 7 describe the analysis using various methods to determine α_s, section 8 describes a test on the gluon spin with both models, and section 9 summarizes the results.

2. Methods to determine α_s

To determine α_s in first order, one has to measure how often a quark radiates a gluon, since

$$\alpha_s = \frac{\sigma(e^+e^- \to q\bar{q}g)}{\sigma(e^+e^- \to q\bar{q})} \alpha \frac{\sigma(e^+e^- \to 3 \text{ jets})}{(e^+e^- \to 2 \text{ jets})} \tag{2}$$

The gluon radiation is given by a Bremsstrahlungsspectrum[6]

$$\frac{d\,\sigma\,(e^+e^- \to q\bar{q}g)}{dk\ \ d\,\theta_g} \alpha \frac{1}{k\ \sin\theta_g} \tag{3}$$

Here k is the gluon energy and θ_g is the angle between gluon and quark flight direction. The cross section diverges for small angles and soft gluons. The problem of measuring α_s looks similar to the measurement of photon bremsstrahlung: one measures only in the region for $k > k_{min}$ and $\theta > \theta_{min}$, where k_{min} and θ_{min} are some minimum gluon energy and emission angle. However, after hadronization k_{min} and θ_{min} are not well defined due to the overlap of the jets. Therefore, one needs elaborate Monte Carlo programs to separate the contributions form $q\bar{q}$ and $q\bar{q}g$ to the observables, from which one wants to determine α_s.

Good observables for the determination of α_s fulfil the following criteria:

a) They are strongly dependent on α_s.
b) They have small contributions from $q\bar{q}$-events.
c) They are insensitive to fragmentation effects.
d) They are calculable in QCD, meaning no infrared divergencies.

We have determined α_s from the following observables:

a) The fraction of 3-jet events selected by various topological cuts.
b) The thrust distribution from events with 3 clusters defined by a cluster algorithm[7].
c) The asymmetry of the energy weighted angular correlation between the final state hadrons[8].

3. Description of the models

In the HM each parton fragments independently according to the FF prescriotion. The gluon is considered randomly either as a quark or an antiquark carrying the total gluon energy. Only mesons are created in the final state.

The fragmentation in the LM is based on the string model[3]. In a $q\bar{q}$ event a colour string is streched between the quark and antiquark. If the q and $\bar{q}$ move in opposite directions, the string breaks up into new quark-antiquark pairs or diquark-antidiquark pairs, which are combined to yield on the average ten primary hadrons (mesons and baryons) at E_{cm} = 34 GeV. In a $q\bar{q}g$ event the gluon is treated like a transverse motion of the string (a "kink"). The string breaks at the position of the kink by splitting off a primary meson. The remaining two strings fragment independently in their own rest frames. Each string piece moves with a velocity $V_i = V_g \sin\alpha_i$ in the laboratory frame (see Figure 1). Boosting the fragmentation products from the restframe to the laboratory frame collimates the primary hadrons into the region between the gluon and quark or antiquark, thus causing a $q\bar{q}g$ event to look more 2-jet like after fragmentation. This lowers the fraction of Monte Carlo generated 3-jet events, thus requiring a higher value of α_s for a given fraction of 3-jet events in the data.

The LM is more "infrared stable" than the HM in the sense that generation of soft or collinear gluons does not change the event shape drastically, but merely introduces some additional transverse momentum (see Fig. 2). The smooth transition between $q\bar{q}$ and $q\bar{q}g$ events allows much softer cuts on the matrix element in the LM than in the HM.

The values of the main parameters and some of the differences between the models are summarized in Table 1.

4. Data analysis

The data used for theis analysis were taken at an average center of mass energy of 34 GeV with the CELLO detector[9]. The analysis was done using charged particles only. The basic cuts for the multihadron selection were the visible energy $E_{vis} > 0.25\ E_{cm}$ and the charge multiplicity larger than 6. All candidates were scanned with an event display,leaving 3021 events with a negligible amount of background.

In order to compare the generated Monte Carlo events with the data, we have processed them through a realistic simulation of our detector and through the selection and reconstruction programs. The parameter σ_q was obtained from the transverse momentum distribution of the charged particles in the slim jet (see Fig.3). We found σ_q = 0.3 GeV/c for both generators. For the longitudinal fragmentation function f(z), we used the original values of the parameters (see Table 2). The ratio of vector- to pseudoscalar mesons V/P was set to 1 . This value provides a good description of the multiplicity distribution, which is sensitive to this ratio (see Fig. 4).

5. Determination of α_s using the fraction of 3-jet events

In order to select mainly 3-jet events we applied shericity (S), aplanarity (A) and oblateness (O) cuts, or we selected events with three reconstructed jets using a cluster algorithm[7]. Three different criteria were used to select the 3-jet events:

1. $S \geqq 0.25$ and $A \leqq 0.1$
2. $O \geqq 0.2$ or $O \geqq 0.3$
3. events with three clusters of particles (jets)

For the criteria 1 and 2, we required at least two particles in each hemisphere defined by the plane perpendicular to the event axis.

We have defined the fraction of 3-jet events f_3 as the fraction of events satisfying one of the above criteria. Besides α_s, this fraction depends on the values of the other parameters of the models, in particular on σ_q, The dependence of f_3 on α_s is shown in Fig. 5 for different values of σ_q. It can be seen that in the LM f_3 is insensitive to σ_q. In the HM f_3 varies more with σ_q. This is probably due to the fact that in the HM σ_q is the only parameter, which determines the transverse spread of a jet. In the LM there are three sources which determine the transverse spread of a jet:

a) The transverse spread of a generated quark, determined by σ_q.
b) The kink in the string for $q\bar{q}g$ events, which gives a transverse momentum to the whole string and therefore to all particles.
c) The many soft or collinear gluons introduce transverse momentum (see Fig.2).

We have also checked that in the LM f_3 is insensitive to the ratio V/P.

Table 2 summarizes the values of α_s obtained with the different topological cuts (only statistical errors are given). The values of α_s obtained with the HM, varying between 0.15 and 0.20, are in good agreement with those measured previously[10] using similar fragmentation models. However, with the LM we find α_s values between 0.24 and 0.28.

We have checked[2] many distributions to see whether both models describe the data in spite of the different values of α_s (a few of these distributions are shown in Figs. 6 - 7). Although the LM gives a better χ^2 in most of the distributions, the difference is not sufficient to exclude one of the models, taking into account that neither of the models gives a perfect description of the data.

To investigate more quantitatively the difference in α_s between the models, we have used the possibility in the Lund program to generate events according to the FF prescription as is done in the HM. We have proceeded in to steps:
In the first step the jets were fragmented independently according to FF. No change was made in the gluon fragmentation. This increases f_3 for the Monte Carlo generated events considerably, as shown in Fig. 8.
In the second step we have in addition treated the gluon as a quark, as in the HM. This increases f_3 again, as shown in Fig. 8 too. The remaining difference between the HM and the LM is attributed to the different treatment of heavy meson decays, the fact that the LM takes quark masses into account in the matrix element, the different cuts to avoid infrared divergencies in the $q\bar{q}g$ generation, the different ways to impose energy conservation in the events, etc.

6. Determination of α_s using the thrust distribution

In this method we measure α_s by selecting the 3-jet events according to the algorithm described in Ref. (7), and by fitting the acceptance corrected thrust distribution of these events to the predictions of the two models. The least square fits yield the following values of α_s:

$$\alpha_s = 0.155 \pm 0.015 \quad \text{for the HM } (\chi^2/DF = 5.0/4)$$
$$\alpha_s = 0.235 \pm 0.025 \quad \text{for the LM } (\chi^2/DF = 9.0/4)$$

This result disagrees with a previous comparison of the models[11]. More detailed information can be found in Ref. (12).

7. Determination of α_s from the energy weighted angular correlations

The angular correlation between hadrons in $q\bar{q}$ events can be demonstrated in a distribution of the angles between all possible pairs of hadrons in an event: such a distribution shows two peaks near 0 and 180 degrees corresponding to the two jets. For $q\bar{q}$ events this distribution is symmetric around 90^0, but $q\bar{q}g$ events fill the region between 0^0 and 180^0 in an asymmetric way, characteristic for gluon bremsstrahlung. If the angular correlations are weighted with the energy of each particle , no infrared divergencies occur. Therefore the energy weighted angular correlations (EWACS) can be calculated in first[8] and second[13] order QCD. The EWACS asymmetry is expected to be fragmentation independent [8].

An experimental determination of EWACS is straightforward: it does not require a separation of 2 and 3 jet events, but it is obtained by simply plotting the angles θ between all pairs of hadrons, labeled i and j and weighting each entry with $z_i z_j$, where z_i and z_j are the fractional energies E_i/E_{cm} and E_j/E_{cm} of the hadrons i and j.

The asymmetry $A(\theta)$ of the EWACS distribution $f(\theta)$ is defined by

$$A(\theta) = f(\pi - \theta) - f(\theta) \tag{4}$$

where

$$f(\theta) = \frac{1}{\sigma}\,\frac{d\sigma}{d\theta} = \frac{1}{\Delta\theta}\,\frac{1}{N}\sum_{k=1}^{N}\sum_{i}\sum_{j} z_i\, z_j\, \delta(\theta_{ij} - \theta) \tag{5}$$

Here N is the number of events and $\Delta\theta$ is the bin width, for which θ_{ij} is taken to be equal to θ. A Monte Carlo study has shown that the contribution from $q\bar{q}$ events to $A(\theta)$ is negligible for $\theta > 20^0$.

To obtain α_s one usually fits $A(\theta)$ from the data to the theoretical QCD formula[14]. However, this is wrong if the final state hadrons have an asymmetry different from the partons. This occurs in the LM, since the boosting of the string considerably reduces the asymmetry of the final state hadrons as compared to the parton asymmetry (see Fig. 9). For the HM the asymmetry is similar for partons and final state hadrons (see Fig. 9).

Therefore we did not fit the theoretical QCD formula to the data, but determined α_s by comparing the asymmetry of the final state hadrons of Monte Carlo events, generated with different values of α_s, with the corrected asymmetry of the data. A least square fit yielded:

$$\alpha_s = 0.15 \pm 0.02 \quad \text{for the HM}$$

and $$\alpha_s = 0.25 \pm 0.04 \quad \text{for the LM.}$$

We have made again a generator study by using the LM without string fragmentation. As shown in Fig. (10) the LM with independent parton fragmentation gives a much higher asymmetry in the final state hadrons than the LM with string fragmentation. For both Monte Carlo generators the angular correlations at the parton level do not agree with the first order QCD formula due to the cuts on the matrix element in the Monte Carlo to avoid the divergent regions. However, this discrepancy cancels in the asymmetry for $\theta > 30^0$, as shown in Fig. (9), where we compared also the QCD predictions with the parton asymmetry of the Monte Carlo generation.

8. Spin test of the gluon

A scalar gluon can be distinguished from a vector gluon by studying the parton thrust (T) distribution, since for a vector gluon[15]

$$\frac{1}{\sigma_0}\frac{d\sigma(q\bar{q}g)}{dT} \simeq \frac{2\alpha_s}{3\pi}\left[\frac{2(3T^2 - 3T + 2)}{T(1 - T)}\ln\left(\frac{2T - 1}{1 - T}\right) - \frac{3(3T - 2)(2 - T)}{1 - T}\right] \tag{6}$$

and for a scalar gluon S[15]

$$\frac{1}{\sigma_0}\frac{d\sigma(q\bar{q}S)}{dT} \simeq \frac{\alpha_s^S}{3\pi}\left[2\ln\left(\frac{2T - 1}{1 - T}\right) + \frac{(4 - 3T)(3T - 2)}{1 - T}\right] \tag{7}$$

where σ_0 is the cross section for $e^+e^- \rightarrow q\bar{q}$ and α_s^S is the coupling constant for a scalar gluon.

The thrust distribution can be obtained from the angles between the jet axis, in 3-jet events, since

$$T = \max(x_i) \text{ with } x_i = 2(\sin\theta_{ij})/(\sin\theta_{12} + \sin\theta_{13} + \sin\theta_{23}) \tag{8}$$

Here θ_{ij} is the angle between the axis of clusters i and j projected onto the event plane.

Up to now the spin tests[16)] have been performed using fragmentation models with independent parton fragmentation, for which the jet axis is a good approximation for the parton axis. This is not necessarily true in a string model and it is interesting to see if the vector gluon is still preferred over a scalar gluon in a string model. Therefore, we have repeated a spin test with both models by comparing the parton thrust with the formulas given in Eqs. (6) and (7). To obtain the parton thrust we corrected the data both with the HM and the LM using their different values of α_s.

A least square fit of the parton thrust with the theoretical QCD formulas yields[12)] for the vector case:

$$\alpha_s = 0.16 \pm 0.015 \quad \text{for the HM} \quad (\chi^2/DF = 2.86)$$
$$\alpha_s = 0.26 \pm 0.015 \quad \text{for the LM} \quad (\chi^2/DF = 3.2)$$

and for the scalar case:

$$\alpha_s^s = 1.28 \qquad \text{for the HM} \quad (\chi^2/DF = 24)$$
$$\alpha_s^s = 3.7 \qquad \text{for the LM} \quad (\chi^2/DF = 24)$$

The best fits are shown in Fig. 11.

The χ^2 values for the scalar case are considerably worse than the corresponding ones for the vector gluon. Therefore, in first order, the vector gluon is clearly preferred over a scalar gluon. However, since α_s^s is large, higher order corrections can be large, but they have not been calculated for a scalar gluon.

9. Conclusion

We have determined the value of the strong coupling constant α_s from the analysis of multihadron events by comparing them with two different models (the model of Hoyer et al. and the Lund model). With the Hoyer model we find α_s values between 0.15 and 0.20, depending on the method used (see Table 2). These values are in good agreement with the previously published values of α_s using first order QCD and independent parton fragmentation[10]. However, with the Lund model we find values of α_s between 0.24 and 0.28. This is mainly attributed to the string fragmentation and to the way the gluon is treated in the Lund model.

At present, neither of the two studied models can be excluded. Therefore we conclude that the systematic uncertainty in α_s is rather large due to our ignorance of the way quarks and gluons produce final state hadrons. Conclusions similar to ours have been published elsewhere[17].

Both models prefer a vector gluon over a scalar gluon, if first order QCD predictions for the parton thrust are compared with the data. However, the strong coupling constant for a scalar gluon is larger than one. Therefore, higher order corrections may be important, but they have not been calculated.

Acknowledgements

I am indebted to my CELLO colleagues for the fine collaboration and many discussions, especially with Drs. A. Gaidot, G. Grindhammer, Y. Lavagne and J.-P. Pansart. I am also indebted to Mrs. B. Klopries for the efficient typing of the manuscript.

References

1) For a general review on experimental evidence for the existence of the gluon see e.g.:
P. Söding and G. Wolf, Ann.Rev.Nucl.Sci. 31(1981)231 and references therein.
2) CELLO Coll., M.J. Behrend et al., DESY Report 82-061, submitted to Nucl.Phys.
3) B. Andersson, G. Gustafson, T. Sjöstrand, Z.Phys. C6(1980)235
T. Sjöstrand, Lund Preprint, LU TP 80-3(1980)
B. Andersson, G. Gustafson, T. Sjöstrand, Nucl.Phys. B197(1982)45
4) P. Hoyer et al., Nucl.Phys. B161(1979)349
5) R.D. Field, R.P. Feynman, Nucl.Phys. B136(1978)1
6) J. Ellis, M.K. Gaillard, G.G. Ross, Nucl.Phys. B111 (1976)253
G. Kramer, G. Schierholz, J. Willrodt, Z.Phys. C4(1980)149
T.A. De Grand, Y.J. Ng, S.N. Tye, PHys.Rev. D16(1977)3251
7) H.J. Daum, H. Meyer, J. Burger, Z.Phys. C8(1981)167
8) C.L. Basham, L.S. Brown, S.D. Ellis, S.T. Love, Phys.Rev.Lett. 41(1978)1585
9) CELLO Coll., H.J. Behrend et al., Phys.Scripta 23(1981)610
10) CELLO Coll., H.J. Behrend et al., Phys.Lett. 110B(1982)329 ; 113B(1982)427
JADE Coll., W. Bartel et al., Phys.Lett. 91B(1980)142
MARK J Coll., D.P. Barber et al., Phys.Lett. 89B(1980)139 and Phys.Lett. 108B(1982)63
PLUTO Coll., Ch. Berger et al., Phys.Lett. 97B(1980)459
TASSO Coll., R. Brandelik et al.,Phys.Lett. 94B(1980)437
11) E. Elsen, PhD Thesis, University of Hamburg (1981)
12) Y. Lavagne, These de 3eme Cycle,University of Paris VII (1982)
13) A. Ali, F. Barreiro, Phys.Lett. 118B(1982)155
D.G. Richards, W.J. Stirling, S.D. Ellis, Phys.Lett. 119B(1982)193
14) PLUTO Coll., Ch. Berger et al., Phys.Lett. 99B(1981)292
MARK II Coll., D. Schlatter et al., Phys.Rev.Lett. 49(1982)521
CELLO Coll., H.J. Behrend et al., Z.Phys. C14(1982)95

15) A. de Rújula, J. Ellis, E.G. Floratos, M.K. Gaillard, Nucl.Phys. B138(1978)387
16) TASSO Coll., R. Brandelik et al., Phys.Lett. 97B(1980)459
PLUTO Coll., Ch. Berger et al., Phys.Lett. 97B(1980)459
CELLO Coll., H.J. Behrend et al, Phys.Lett. 110B(1982)329
17) R.D. Field, Lecture given at the Conference on perturbative QCD, publ. in: Brookhaven 1981 Proceedings, Isabelle Vol. 1,11-73
R.D. Field, S. Wolfram, Preprint UFTP 82-12(1982)
S.D. Ellis, talk given at the XXI Int. Conference on High Energy Physics, Paris, July 1982.

Table 1: Main characteristics of the Monte Carlo models

Parton generation	1^{st} order QCD cuts on fractional parton energies taking quark masses into account	1^{st} order QCD maximum fractional energy of parton = 0.97 minimum parton energy = 2 GeV
Generation of primary quark pairs	uu:dd:ss:cc =3:3:1:0	uu:dd:ss:cc:=2:2:1:0
Longitudinal fragmentation function $z = \frac{(E + P_z)_{meson}}{(E + P_z)_{quark}}$	$f(z) = (1+a)(1-z)^a$ a decreases with quark mass (0.5 for u, 0.09 for b)	$f(z) = 1-a+3a(1-z)^2$ a = 0.77 for u, d, s a = 0 for c and b a = 1 for gluon
Transverse momentum of primary quarks	gaussian with σ_q = 0.3 GeV/c	gaussian with σ_q = 0.3 GeV/c
Gluon fragmentation	gluon splits into 2 $q\bar{q}$ pairs with each half of the gluons energy	gluon splits into 1 $q\bar{q}$ pair with one quark taking all of the energy
Ratio of vector- to pseudo scalar mesons	V/P = 1	V/P = 1
Generation of diquarks	yes, leading to baryons	no

Table 2: Value of α_s obtained at $\sqrt{s}$ = 34 GeV with the Lund model (LM) and the Hoyer model (HM) (first order QCD).
The error in the determination of α_s using the 3 jet fraction (see text) is statistical only (including statistical Monte Carlo error).

Method	Lund model	Hoyer model	$\frac{\alpha_s\ (LM)}{\alpha_s\ (HM)}$
$S \geq 0.25 \quad A \leq 0.1$	0.280 ± 0.045	0.190 ± 0.030	1.47
$O \geq 0.20$	0.260 ± 0.040	0.190 ± 0.020	1.37
$O \geq 0.30$	0.255 ± 0.050	0.200 ± 0.035	1.28
# of 3-jet events	0.235 ± 0.025	0.145 ± 0.020	1.62
Cluster Thrust	0.235 ± 0.025	0.155 ± 0.015	1.52
EWACS*	0.250 ± 0.040	0.150 ± 0.020	1.67

*Energy Weighted Angular Correlations

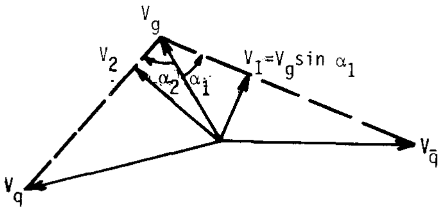

Fig. 1 The kinematics of a $q\bar{q}g$ system. The vectors V_q, $V_{\bar{q}}$, and V_g give the velocities of the outgoing partons. The vectors V_1 and V_2 give the velocities of the string pieces in the laboratory frame.

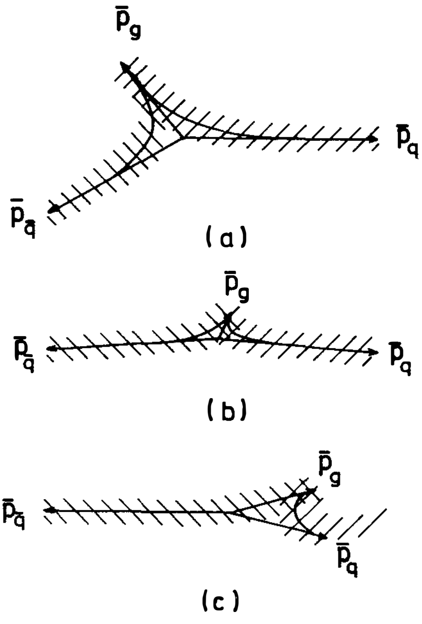

Fig. 2 The momentum distribution of mesons in $q\bar{q}g$ events. In Fig. 1a the typical distribution along two hyperbolas is shown, where the hatched areas indicate the broadening coming from differences in mass and transvers momentum. In Figs. 1b and 1c the corresponding structures are shown for a weak and a collinear gluon, respectively[3].

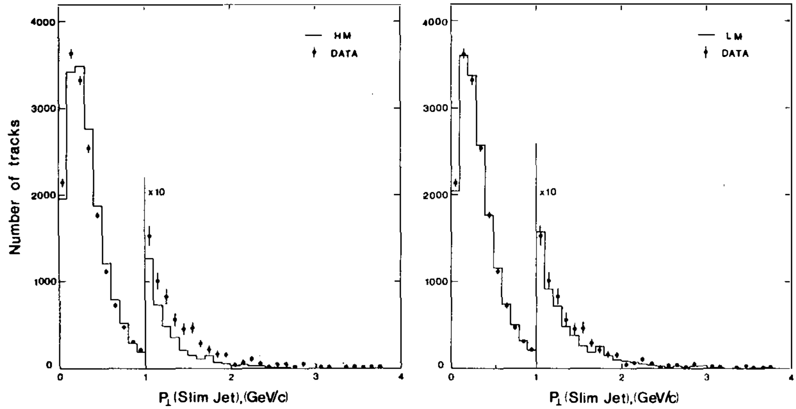

Fig. 3 The transverse momentum distribution of charged particles of the slim jet with respect to its sphericity axis compared with both models.

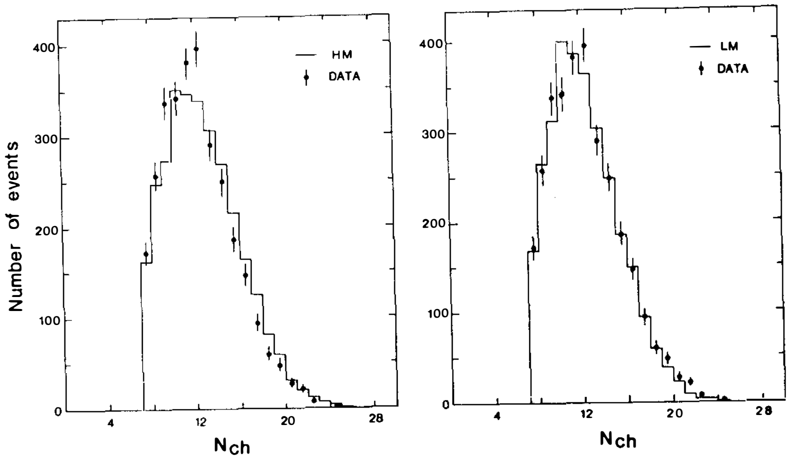

Fig. 4 The charged multiplicity for events with xvis 0.25 compared with both models.

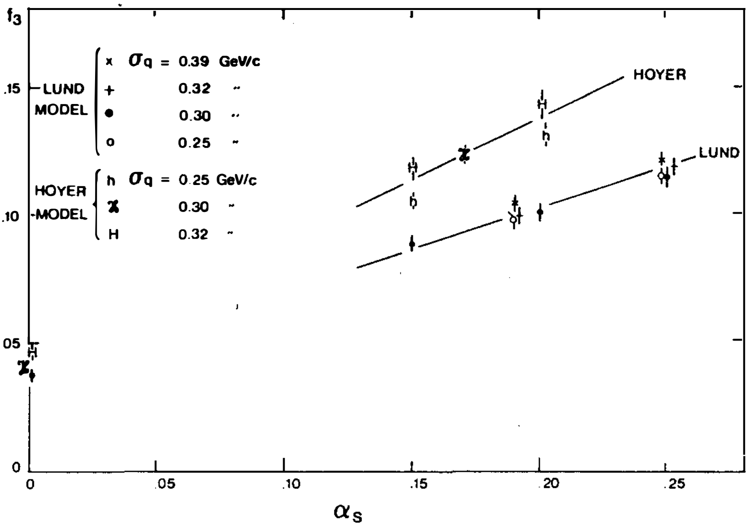

Fig. 5 Monte Carlo prediction for the fraction of 3-jet events f_3 versus α_s for different values of σ_q. Note that for the Lund model f_3 is appreciably smaller than f_3 for the Hoyer model for a given α_s.

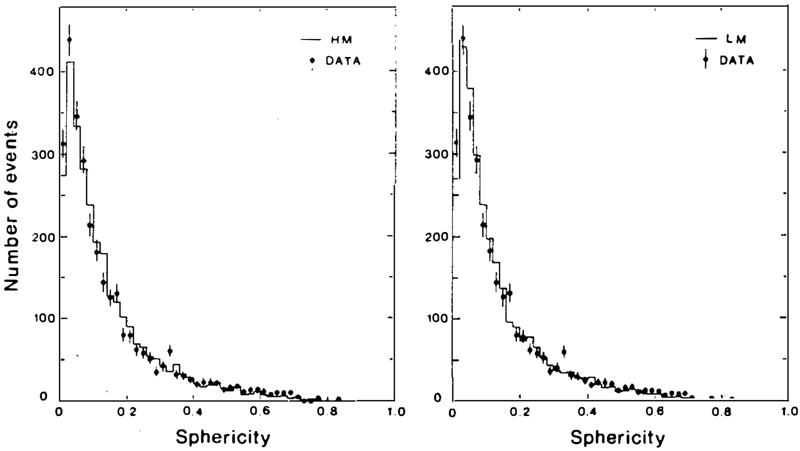

Fig. 6 The sphericity distribution compared with the two Monte Carlo models.

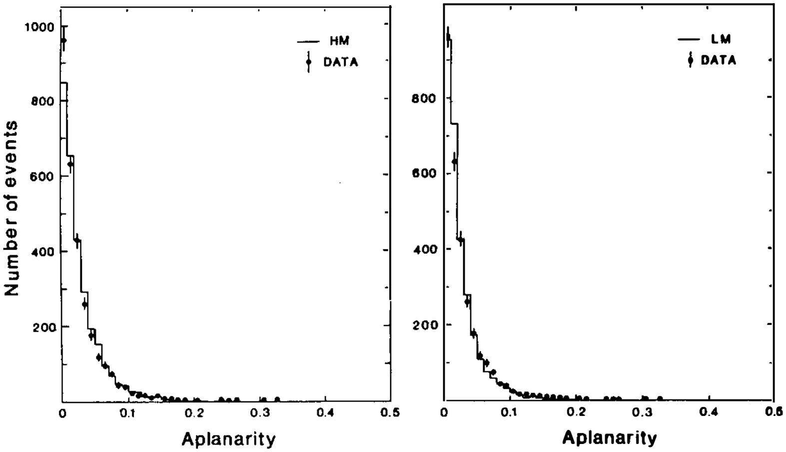

Fig. 7 The aplanarity distribution compared with both Monte Carlo models.

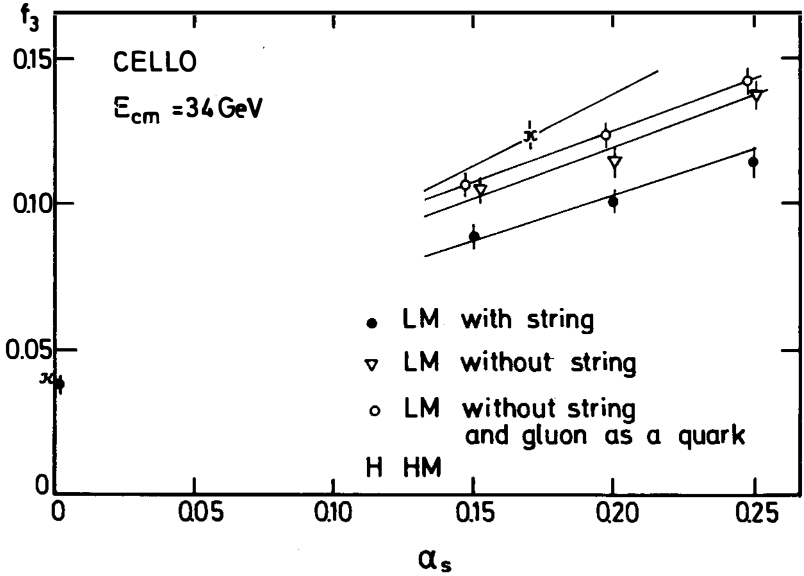

Fig. 8 Generator study of f_3 versus α_s for different fragmentation conditions. f_3 is the fraction of events with $S \geq 0.25$ and $A \leq 0.1$.

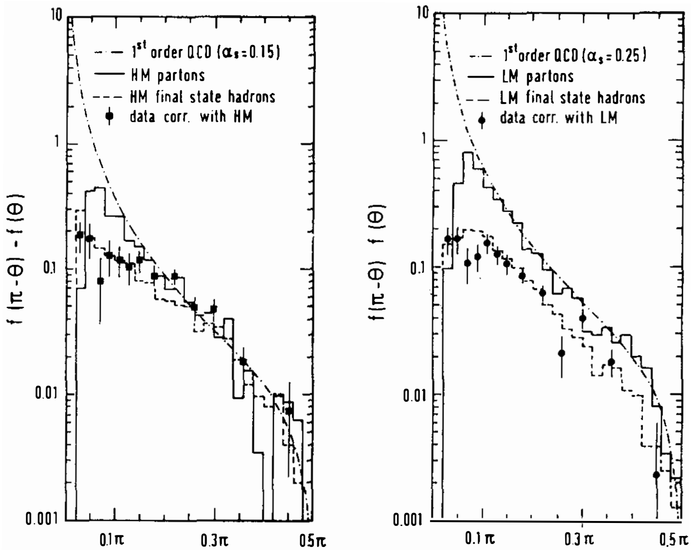

Fig. 9 Asymmetry of the energy weighted angular correlations at 34 GeV.

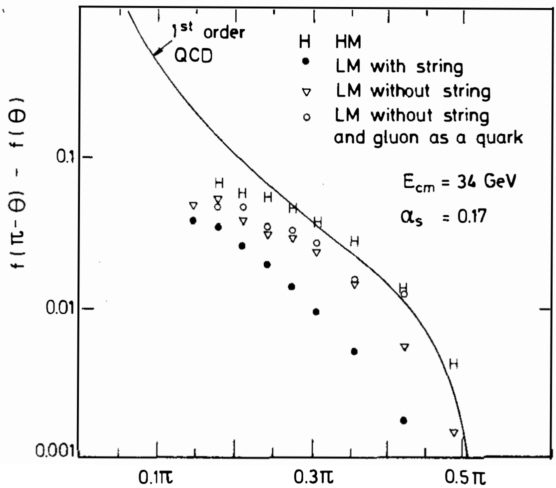

Fig. 10 Generator study of the asymmetry for different fragmentation conditions.

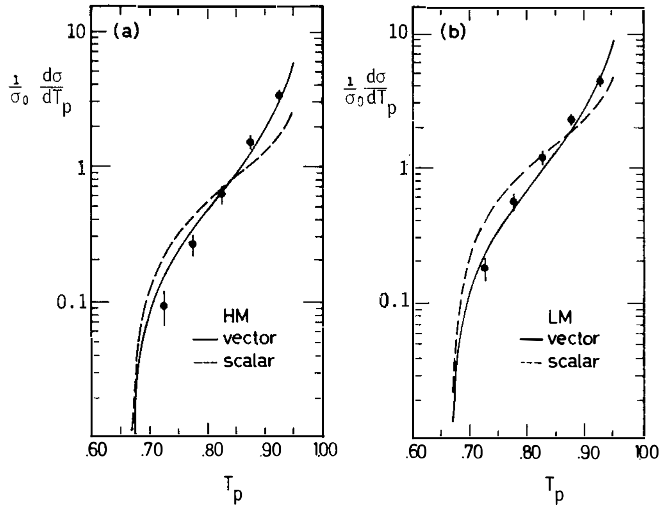

Fig. 11 The parton thrust of 3-jet events compared with a vector gluon and scalar gluon theory.